PROCEEDINGS OF SCIENCE

Modified HQET power counting for constrained second-order power corrections in $B \to D^{(*)} l \nu$: $R(D^{(*)})$, $|V_{cb}|$ and New Physics

Florian U. Bernlochner,[a] **Zoltan Ligeti,**[b,c] **Michele Papucci,**[d] **Markus T. Prim,**[a,*] **Dean J. Robinson**[b,c] **and Chenglu Xiong**[a]

[a] *Physikalisches Institut der Rheinischen Friedrich-Wilhelms-Universität Bonn, 53115 Bonn, Germany*
[b] *Ernest Orlando Lawrence Berkeley National Laboratory, University of California, Berkeley, CA 94720, USA*
[c] *Berkeley Center for Theoretical Physics, Department of Physics, University of California, Berkeley, CA 94720, USA*
[d] *Walter Burke Institute for Theoretical Physics, California Institute of Technology, Pasadena, CA 91125, USA*

E-mail: markus.prim@cern.ch

We develop a modified power-counting within the heavy quark effective theory (HQET), that results in a highly constrained set of second-order power corrections in the heavy quark expansion, compared to the standard approach. We implement this modified expansion to determine all $\bar{B} \to D^{(*)}$ form factors, both within and beyond the Standard Model, to $O(\alpha_s, \alpha_s/m_{c,b}, 1/m_{c,b}^2)$. Using measured $\bar{B} \to D^{(*)}\ell\bar{\nu}$ differential branching fractions for light leptons ($\ell = e, \mu$), we constrain not only leading and subleading Isgur-Wise functions, but also the $1/m_{c,b}^2$ corrections from subsubleading terms. We provide updated precise predictions for $\bar{B} \to D^{(*)}\tau\bar{\nu}$ decay rates, lepton universality ratios, and the CKM matrix element $|V_{cb}|$.

41st International Conference on High Energy physics - ICHEP2022
6-13 July, 2022
Bologna, Italy

*Speaker

PoS(ICHEP2022)758

1. Introduction

We present form factors for $\bar{B} \to D$ and $\bar{B} \to D^*$ transitions developed in the framework of the heavy quark effective theory (HQET), used in studying matrix elements involving hadrons containing a single charm or bottom quark. Form factor parametrizations based on HQET allow for hadronic model-independent, high-precision determinations of the CKM matrix element $|V_{cb}|$ from fits to the differential measurements of the exclusive semileptonic decays $\bar{B} \to D^{(*)}\ell\bar{\nu}$, ($\ell = e, \mu$). Furthermore, HQET allows for model-independent precise predictions for observables sensitive to physics beyond the Standard Model (SM). In the following, we give a brief overview of our results. A more thorough write-up can be found in Ref. [1], and a prior study in Ref. [2]. An implementation of the presented material is available in the HAMMER library [3, 4].

2. $\bar{B} \to D^{(*)}$ Form Factors

The hadronic transitions $\bar{B} \to D^{(*)}$ are described by two (four) form factors in the SM. The key idea is to express the $\bar{B} \to D^{(*)}$ form factors $\hat{h}(w) = h(w)/\xi(w)$, which are a function of the hadronic recoil w, in leading $\xi(w)$ and sub-leading $O(1/m_{\mathrm{b,c}}^{(2)})$ and $O(1/(m_{\mathrm{b}}m_{\mathrm{c}}))$ Isgur-Wise (IW) functions via the heavy quark expansion. The leading-order IW function is parametrized as a polynominal

$$\frac{\xi(w)}{\xi(w_0)} = 1 - 8a^2\rho_*^2 z_* + 16(2c_* a^4 - \rho_*^2 a^2) z_*^2 + \ldots \tag{1}$$

in the optimized conformal variable

$$z_*(w) = \frac{\sqrt{w+1} - \sqrt{2}a}{\sqrt{w+1} + \sqrt{2}a}\,, \quad \text{with} \quad a^2 \equiv \frac{w_0 + 1}{2} = \frac{1 + r_D}{2\sqrt{r_D}}\,. \tag{2}$$

The current experimental and lattice data have no sensitivity to cubic terms in $\xi(w)$ when sub-leading IW functions are included. In the following, the $\hat{L}_i^{((n))}$ and $\hat{M}_i$ are expressed as linear combinations of higher-order IW functions normalized to $\xi(w)$. For a compact notation we define $\hat{L}_i^{((Q))} = \hat{L}_i^{((1))} + \epsilon_Q \hat{L}_i^{((2))}, Q = c, b$. In this notation, the hatted SM $\bar{B} \to D$ form factors at second-order are:

$$\begin{aligned} \hat{h}_+ &= 1 + \hat{\alpha}_s \left[C_{V_1} + \frac{w+1}{2}\,(C_{V_2} + C_{V_3}) \right] + \sum_{Q=c,b} \varepsilon_Q \hat{L}_1^{(Q)} - \varepsilon_c \varepsilon_b \hat{M}_8\,, \\ \hat{h}_- &= \hat{\alpha}_s\,\frac{w+1}{2}\,(C_{V_2} - C_{V_3}) + \varepsilon_c \hat{L}_4^{(c)} - \varepsilon_b \hat{L}_4^{(b)}\,, \end{aligned} \tag{3}$$

and the the hatted SM $\bar{B} \to D^*$ form factors at second-order are:

$$\begin{aligned} \hat{h}_V &= 1 + \hat{\alpha}_s\, C_{V_1} + \varepsilon_c \big[\hat{L}_2^{(c)} - \hat{L}_5^{(c)}\big] + \varepsilon_b \big[\hat{L}_1^{(b)} - \hat{L}_4^{(b)}\big] + \varepsilon_c \varepsilon_b \hat{M}_9\,, \\ \hat{h}_{A_1} &= 1 + \hat{\alpha}_s\, C_{A_1} + \varepsilon_c \left(\hat{L}_2^{(c)} - \hat{L}_5^{(c)}\,\frac{w-1}{w+1}\right) + \varepsilon_b \left(\hat{L}_1^{(b)} - \hat{L}_4^{(b)}\,\frac{w-1}{w+1}\right) + \varepsilon_c \varepsilon_b \hat{M}_9\,, \\ \hat{h}_{A_2} &= \hat{\alpha}_s\, C_{A_2} + \varepsilon_c \big[\hat{L}_3^{(c)} + \hat{L}_6^{(c)}\big] - \varepsilon_c \varepsilon_b \hat{M}_{10}\,, \\ \hat{h}_{A_3} &= 1 + \hat{\alpha}_s \big(C_{A_1} + C_{A_3}\big) + \varepsilon_c \big[\hat{L}_2^{(c)} - \hat{L}_3^{(c)} + \hat{L}_6^{(c)} - \hat{L}_5^{(c)}\big] + \varepsilon_b \big[\hat{L}_1^{(b)} - \hat{L}_4^{(b)}\big] \\ &\qquad + \varepsilon_c \varepsilon_b \big[\hat{M}_9 + \hat{M}_{10}\big]\,, \end{aligned} \tag{4}$$

HQET order	IW functions		
	All	RC Expansion	VC Limit
$1/m^0_{c,b}$	1	1	1
$1/m^1_{c,b}$	3	3	1
$1/m^2_{c}$	20	1	3
$1/m^2_{c,b}$	32	3	4

Table 1: Number of $\bar{B} \to D^{(*)}$ form factors and IW functions entering at each fixed order in HQET.

Including second-order corrections increases the number of IW functions to a total of 32. We study two approaches to reduce the number of IW functions: 1. A supplemental power counting in θ for HQET based on power counting in the transverse residual momentum $\not{D}_\perp$, the *residual chiral expansion* (RC). In the low energy effective theory, this corresponds to counting the number of operator products inserted along the heavy quark line. The form factors in Eq. 3 and Eq. 4 are given at θ^2 in this power counting. 2. The *vanishing chromomagnetic limit* (VC) $G_{\alpha\beta} \to 0$. The reduction of number of free IW functions is shown in Tab. 1. In the following, we only show an overview of the results in the RC and refer the reader to [1] for a more exhaustive discussion on the results in the RC and also the VC.

3. Fits

We use the differential measurement of the hadronic recoil w distributions of $\bar{B} \to D\ell\nu$ from Ref. [5] ('Belle 15') and the two differential measurements of w of $\bar{B}^0 \to D^{*+}\ell\nu$ from Ref. [6] ('Belle 17') and Ref. [7] ('Belle 19'). Here, we include the well-known lattice results for the $\bar{B} \to D\ell\nu$ decay form factors from Ref. [8, 9], and the $\bar{B} \to D^*\ell\nu$ zero-recoil form factors from Ref. [10]. A more thorough discussion of the impact of the $\bar{B} \to D^*\ell\nu$ beyond zero-recoil form factors can be found in [1].

The free parameters in our model can be separated into two categories: entering at zero recoil are $|V_{cb}|$, m_b^{1S}, δm_{bc}, ρ_1, λ_2, ρ_*^2, c_*, $\hat{\eta}(1)$, and beyond are $\hat{\eta}'(1)$, $\hat{\chi}_2(1)$, $\hat{\chi}_2'(1)$, $\hat{\chi}_3'(1)$, $\hat{\varphi}_1'(1)$, $\hat{\beta}_2(1)$, $\hat{\beta}_3'(1)$. We perform a nested hypothesis test (NHT) [11] to determine the optimal set of fit parameters. The starting point of the NHT is the set of parameters contributing only at zero-recoil. In subsequent fits we add additional parameters in our model in all possible combinations, rejecting an alternative hypothesis if $\Delta\chi^2 < \chi^2_N - \chi^2_{N-1} < 1$ or if the newly introduced parameter is highly correlated. The NHT yields 8 different scenarios which are tabulated in Tab. 2.

Although the allowed models differ in the included combinations of IW functions, the results on V_{cb} are stable. The fitted shapes and form factors of our nominal scenario S1, which has the smallest χ^2 with fewest model parameters, is shown in Fig. 1.

4. Prediction for $R(D^{(*)})$, Biases, and the Major Axis of Doom

With the fitted Bernlochner-Ligeti-Papucci-Robinson-Xiong-Prim (BLPRXP) form factors [1] we can make predictions for the lepton flavor universality ratio $R(D^{(*)})$ using the

$$\text{BLPRXP}: R(D) = 0.288(4)\,, \quad (D^*) = 0.249(1)\,, \quad \rho = 0.12\,. \tag{5}$$

PoS(ICHEP2022)758

Params	$S1$	$S2$	$S3$	$S4$	$S5$	$S6$	$S7$	$S8$
$\lvert V_{cb}\rvert \times 10^3$	38.70(62)	38.90(64)	38.70(68)	38.70(68)	38.70(69)	38.70(67)	38.80(68)	38.70(69)
ρ_*^2	1.10(4)	1.15(4)	1.19(5)	1.15(5)	1.15(4)	1.10(7)	1.12(8)	1.10(4)
c_*	2.39(18)	2.44(19)	2.16(24)	2.25(23)	2.29(29)	2.38(19)	2.41(20)	2.40(29)
$\hat{\chi}_2(1)$	−0.12(2)	−0.14(3)	—	—	−0.12(5)	—	−0.13(4)	−0.12(5)
$\hat{\chi}_2'(1)$	—	—	−0.15(8)	−0.08(7)	−0.07(11)	—	—	0.00(10)
$\hat{\chi}_3'(1)$	—	—	0.04(1)	0.04(1)	—	0.04(1)	—	—
$\hat{\eta}(1)$	0.34(4)	0.33(4)	0.34(4)	0.34(4)	0.34(4)	0.34(4)	0.34(4)	0.34(4)
$\hat{\eta}'(1)$	—	0.12(10)	0.14(11)	—	0.15(11)	−0.15(14)	0.05(19)	—
m_b^{1S} [GeV]	4.71(5)	4.71(5)	4.70(5)	4.70(5)	4.71(5)	4.71(5)	4.71(5)	4.71(5)
δm_{bc} [GeV]	3.41(2)	3.41(2)	3.41(2)	3.41(2)	3.41(2)	3.41(2)	3.41(2)	3.41(2)
$\hat{\beta}_2(1)$	—	—	—	—	—	—	—	—
$\hat{\beta}_3'(1)$	—	—	—	—	—	—	—	—
$\hat{\varphi}_1'(1)$	0.25(21)	—	—	0.24(21)	—	0.53(31)	0.17(40)	0.25(21)
λ_2 [GeV^2]	0.12(2)	0.12(2)	0.12(2)	0.12(2)	0.12(2)	0.12(2)	0.12(2)	0.12(2)
ρ_1 [GeV^3]	−0.36(24)	−0.35(24)	−0.37(24)	−0.36(24)	−0.37(24)	−0.36(24)	−0.36(24)	−0.36(24)
χ^2	29.8	30.0	28.9	29.3	29.5	29.6	29.8	29.8
ndf	31	31	30	30	30	30	30	30
ρ^2	1.35(5)	1.37(5)	1.34(6)	1.34(6)	1.34(6)	1.34(6)	1.36(6)	1.35(6)
c	2.41(17)	2.43(17)	2.14(22)	2.26(21)	2.29(28)	2.40(17)	2.42(17)	2.42(27)

Table 2: Fit values and parameters for each terminating node of the nested hypothesis test graph. The node $S1$ (dark gray) is chosen as the optimal fit hypothesis. To characterize possible model dependence in the parameter truncation, we also consider $S3$ (light gray). The last four rows show the corresponding values for the fit χ^2, number of degrees of freedom, and the slope and the curvature of $\xi(w)$ at zero recoil.

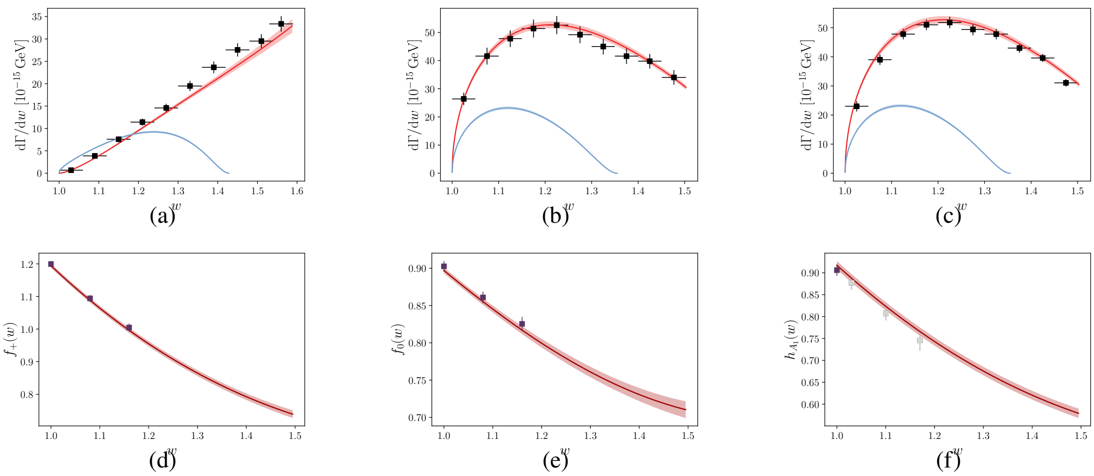

Figure 1: The spectra and form factors (red bands) recovered from the $L^{D;D^*}_{w\geq 1;=1}$ fit scenario in the RC expansion, compared to the fitted experimental data (black markers) and LQCD data (plum markers): (a) $d\Gamma[\bar{B} \to D\ell\nu]/dw$ (Belle 2015); (b) $d\Gamma[\bar{B} \to D^*\ell\nu]/dw$ (Belle 2017); (c) $d\Gamma[\bar{B} \to D^*\ell\nu]/dw$ (Belle 2019); (d) $f_+(w)$; (e) $f_0(w)$; and (f) $h_{A_1}(w)$. Also shown are the corresponding $\bar{B} \to D^{(*)}\tau\nu$ spectra (blue bands). For $h_{A_1}(1) = \mathcal{F}(1)$ the zero recoil prediction of Ref. [12] is used. The beyond zero recoil lattice points for h_{A_1} from Ref. [10], which are not included in this fit, are shown as gray markers.

We find that our prediction is robust when including beyond zero-recoil lattice input for $\bar{B} \to D^*\ell\nu$ and input from QCD sum rules. A noticeable feature is the 2.7σ shift in the predicted values for $R(D^{(*)})$ when comparing to the prediction using the Bernlochner-Ligeti-Papucci-Robinson (BLPR) [2] form factors at first order:

$$\text{BLPR}: R(D) = 0.298(3)\,, \quad (D^*) = 0.261(4)\,, \quad \rho = 0.19\,. \tag{6}$$

We identify two sources of external biases causing this effect: The tension using only 'Belle 17' data vs using 'Belle 17+19' data, and the CLN major-axis approximation. In the CLN type parametriza-

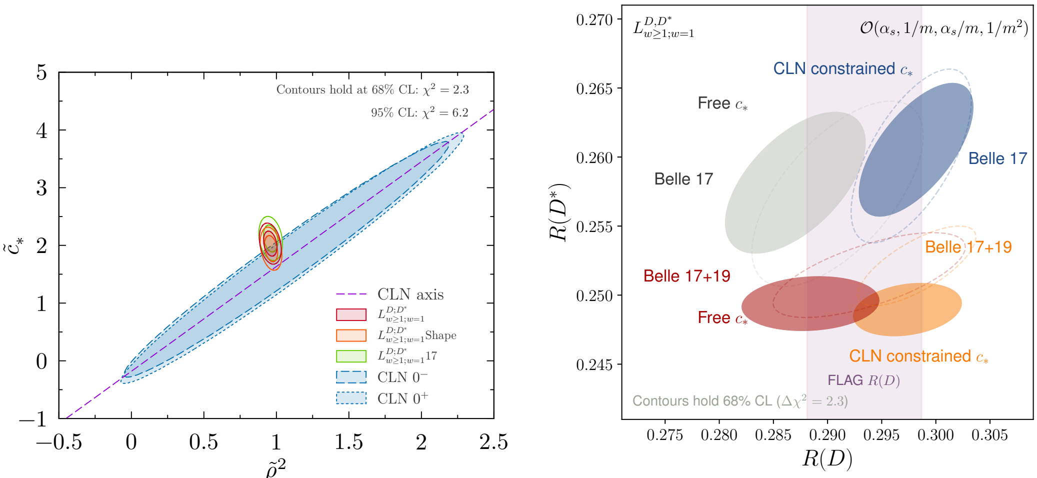

(a) (b)

Figure 2: Left (a): The allowed-region ellipses (blue) arising from dispersive bounds plus unitarity constraints applied to the $\bar{B} \to D$ form factor $\mathcal{G}(w)$ [13]. The major axis of the tighter ellipse, corresponding to the $J^P = 0^-$ current, is shown by the dashed purple line. Also shown are the recovered CLs for various fit scenarios. Right (b): The $R(D^{(*)})$ predictions using different sets of inputs and assumptions. The blue versus gray (orange versus red) ellipses demonstrate the shift in the predicted $R(D)$ when the CLN constraint on c_* is applied versus lifted. The inclusion of the Belle 2019 data results in a reduction of the central value and uncertainty of $R(D^*)$ (gray versus red or blue versus orange ellipses). The light-purple band shows the $R(D)$ LQCD prediction [12]. The dashed lines correspond to the result at first order.

tion, dispersive bounds from unitarity constraints can be applied to $\mathcal{G}(w)$. This constrains the allowed parameter space in the slope-curvature ($\tilde{\rho}^2_*$–$\tilde{c}_*$) plane. In the Caprini-Lellouch-Neubert (CLN) parametrization, the constraint is approximated by the major axis to enforce a linear relationship between $\tilde{\rho}^2_*$ and $\tilde{c}_*$. However, the precision of the available experimental and LQCD data has become precise enough to resolve the minor axis. Thus, this relation introduces a bias in the fits. The so-called major axis of doom and the resulting biases from it and the tension in the experimental data are shown in Fig. 2.

5. Summary

We present second order ($\mathcal{O}(1/m_{c,b}, 1/m^2_{c,b}, 1/(m_c m_b), \alpha_s/m_{c,b})$) corrections for the BLPR [2] form factors: BLPRXP [1]. The key idea to reduce the large number of unconstrained IW functions is a supplemental power counting in θ for HQET based on the transverse residual momentum $\not{D}_\perp$: the residual chiral (RC) expansion. Truncating the RC expansion at $\mathcal{O}(\theta^2)$ leads to a dramatic simplification in HQET. We performed a comprehensive analysis of the available experimental and LQCD data and are able to determine the unconstrained IW functions reliably. We identify a significant shift when making predictions at second order in comparison to first order for the lepton flavor universality ratio $R(D^{(*)})$. This shift is not a feature of the second-order corrections, but can be attributed to two existing biases: a tension in the available experimental data, and the major axis of doom, which both causes significant biases in $R(D^{(*)})$.

6. Acknowledgements

FB is supported by DFG Emmy-Noether Grant No. BE 6075/1-1 and BMBF Grant No. 05H21PDKBA. FB thanks LBNL for its hospitality. MP is supported by the U.S. Department of Energy, Office of Science, Office of High Energy Physics, under Award No. DE-SC0011632 and by the Walter Burke Institute for Theoretical Physics. MTP is supported by the Argelander Starter-Kit Grant of the University of Bonn and BMBF Grant No. 05H21PDKBA. ZL and DJR are supported by the Office of High Energy Physics of the U.S. Department of Energy under Contract No. DE-AC02-05CH11231.

References

[1] F.U. Bernlochner, Z. Ligeti, M. Papucci, M.T. Prim, D.J. Robinson and C. Xiong, *Constrained second-order power corrections in HQET: $R(D^{(*)})$, $|V_{cb}|$, and new physics*, 2206.11281.

[2] F.U. Bernlochner, Z. Ligeti, M. Papucci and D.J. Robinson, *Combined analysis of semileptonic B decays to D and D^*: $R(D^{(*)})$, $|V_{cb}|$, and new physics*, Phys. Rev. D **95** (2017) 115008 [1703.05330].

[3] F.U. Bernlochner, S. Duell, Z. Ligeti, M. Papucci and D.J. Robinson, *Das ist der HAMMER: Consistent new physics interpretations of semileptonic decays*, Eur. Phys. J. C **80** (2020) 883 [2002.00020].

[4] F.U. Bernlochner, S. Duell, Z. Ligeti, M. Papucci and D.J. Robinson, *HAMMER - Helicity Amplitude Module for Matrix Element Reweighting*, Aug., 2022. 10.5281/zenodo.7007837.

[5] Belle Collaboration collaboration, *Measurement of the decay $B \to D\ell\nu_\ell$ in fully reconstructed events and determination of the Cabibbo-Kobayashi-Maskawa matrix element $|V_{cb}|$*, Phys. Rev. **D93** (2016) 032006 [1510.03657].

[6] Belle Collaboration collaboration, *Precise determination of the CKM matrix element $|V_{cb}|$ with $\bar{B}^0 \to D^{*+}\,\ell^-\,\bar{\nu}_\ell$ decays with hadronic tagging at Belle*, 1702.01521.

[7] Belle Collaboration collaboration, *Measurement of the CKM matrix element $|V_{cb}|$ from $B^0 \to D^{*-}\ell^+\nu_\ell$ at Belle*, Phys. Rev. D **100** (2019) 052007 [1809.03290].

[8] Fermilab Lattice and MILC Collaborations collaboration, *$B \to D\ell\nu$ form factors at nonzero recoil and $|V_{cb}|$ from 2+1-flavor lattice QCD*, Phys. Rev. D **92** (2015) 034506 [1503.07237].

[9] HPQCD Collaboration collaboration, *$B \to Dl\nu$ form factors at nonzero recoil and extraction of $|V_{cb}|$*, Phys. Rev. D **92** (2015) 054510 [1505.03925].

[10] Fermilab Lattice and MILC Collaborations collaboration, *Semileptonic form factors for $B \to D^*\ell\nu$ at nonzero recoil from 2 + 1-flavor lattice QCD*, 2105.14019.

[11] F.U. Bernlochner, Z. Ligeti and D.J. Robinson, *$N = 5, 6, 7, 8$: Nested hypothesis tests and truncation dependence of $|V_{cb}|$*, Phys. Rev. D **100** (2019) 013005 [1902.09553].

[12] Flavour Lattice Averaging Group collaboration, *FLAG Review 2021*, 2111.09849.

[13] I. Caprini, L. Lellouch and M. Neubert, *Dispersive bounds on the shape of anti-B —> D(*) lepton anti-neutrino form-factors*, Nucl. Phys. **B530** (1998) 153 [hep-ph/9712417].